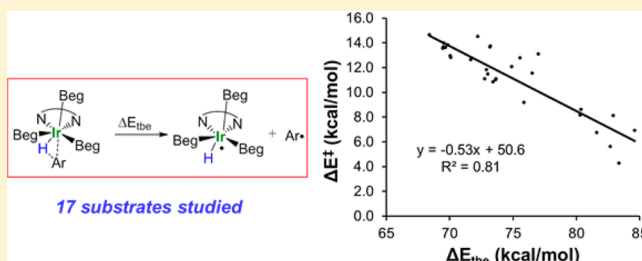# Distortion/Interaction Analysis Reveals the Origins of Selectivities in Iridium-Catalyzed C−H Borylation of Substituted Arenes and 5-Membered Heterocycles

Aaron G. Green, Peng Liu, Craig A. Merlic,* and K. N. Houk*

Department of Chemistry and Biochemistry, University of California, Los Angeles, California 90095, United States

Ⓢ *Supporting Information*

ABSTRACT: The iridium-catalyzed borylation of mono- and disubstituted arenes and heteroarenes has been studied with density functional theory. The distortion/interaction model was employed to understand the origins of selectivities in these reactions. Computations revealed that the transition states for C−H oxidative addition are very late, resembling the aryl iridium hydride intermediate with a fully formed Ir−C bond. Consequently, the regioselectivity is mainly controlled by differences in the interaction energies between the iridium catalyst and arene carbon.

■ INTRODUCTION

Selective functionalization of aromatic C−H bonds is an important approach for the synthesis of complex organic molecules.[1,2] The regioselective borylation of $C(sp^2)$−H bonds is a particularly attractive target because of the well-known utility of arylboron starting materials in a variety of synthetic applications.[3,4] Recently, iridium-catalyzed borylation of aromatic compounds has emerged as a viable alternative to well-known palladium-catalyzed borylations.[5−7] A common borylation protocol involves the use of $[Ir(OMe)(COD)]_2$ as a catalyst precursor with dtbpy (dtbpy = 4,4′-di-*tert*-butyl-2,2′-bipyridine) as the ligand and either bis(pinacolato)diboron (B_2pin_2) or pinacolborane (HBpin) as the boron source (Scheme 1). Experimental studies by Hartwig and co-workers utilizing

$Ir(dtbpy)(Bpin)_3(COE)$ (COE = cyclooctene) as a precatalyst support a mechanism where $Ir^{III}(dtbpy)(Bpin)_3$ is the active catalyst that mediates C−H cleavage via rate-limiting oxidative addition (step i).[8] Subsequent reductive elimination (step ii) yields the arylboronate ester. In this mechanism, regeneration of the active catalyst can occur with either HBpin or B_2pin_2 (steps iii and iv). This mechanism has been supported computationally.[9]

Despite remarkable progress in the use of iridium catalysts, the origins of regioselectivity in this reaction are not well understood.[10] For example, in the case of substituted arenes, the regioselectivity appears to be largely controlled by steric factors. Monosubstituted benzene rings react nearly exclusively at the meta and para positions and the regioselectivity is only slightly perturbed by changing the electronic properties of the substituent (Figure 1).[11−13] Additionally, in the case of 1,2-disubstituted benzene rings, no 3- or 6-borylated products are observed. The selectivity for the 4- or 5-position is influenced by

Scheme 1. Catalytic Cycle for the Iridium-Catalyzed Borylation of Aromatic Rings
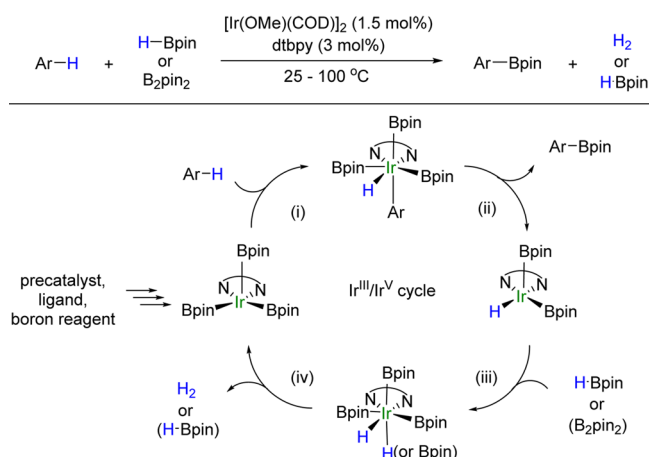
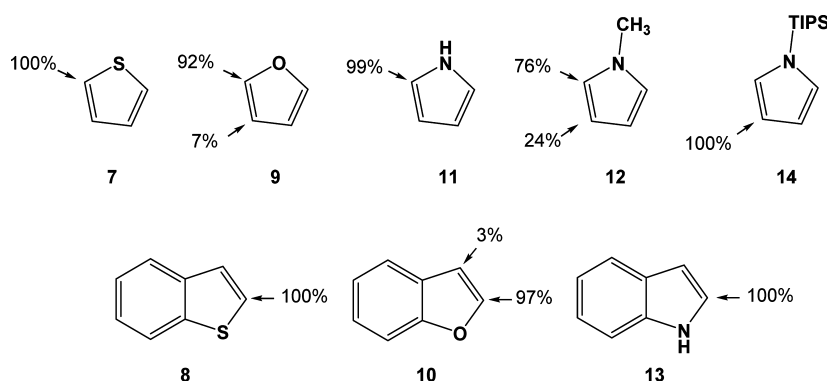**Figure 1.** Regioselectivities of various substituted benzene rings.

Figure 2. Regioselectivities of C−H activation of select 5-membered heterocycles.

electronic properties and the preferred site of C−H activation is para to the weaker electron-donating substituent (Figure 1).[14]

Experimental selectivities for a select group of 5-membered and benzo-fused 5-membered heterocycles **7−14** are shown in Figure 2. Unsubstituted 5-membered heterocycles react exclusively at the 2-position, suggesting a strong electronic effect with these substrates[12,13,15] Only with the presence of a sterically hindering group at the heteroatom does the regioselectivity begin to favor the 3-position.[16] In the case of pyrrole derivatives, reaction with *N*-methylpyrrole yields a mixture of 2- and 3-borylated products. In the presence of a bulky TIPS group at the nitrogen, the reaction of **14** occurs at the 3-position exclusively.[16]

A number of factors may contribute to the reactivity of C−H bonds in the oxidative addition transition states, such as steric effects, the homolytic or heterolytic dissociation energies of the C−H bond, and the stability of the forming Ir−C bond. Recent studies by Maleczka, Singleton, and Smith suggest that the regioselectivity of iridium-catalyzed borylation is governed by the pK$_a$'s of the C−H bond; in the absence of external factors, the most acidic bonds are borylated preferentially.[17] A recent study on iridium-catalyzed borylation by Marder and co-workers also demonstrated that pK$_a$'s of the C−H bonds may provide an indicator of selectivity.[14] However, while some success predicting the preferred borylation position was achieved using NMR spectroscopy, the correlation between calculated substrate pK$_a$ values and selectivity is not perfect.[14] Interestingly, recent computational studies on palladium-catalyzed C−H activations have demonstrated a correlation between regioselectivity and Pd−C bond strengths of the aryl palladium intermediates or C−H activation transition structures. Eisenstein and Perutz et al. found a better correlation between Pd−C bond dissociation energy (BDE) of the reaction intermediates and the activation energy in the direct arylation of fluorinated benzenes than the correlation between pK$_a$ and activation energy.[18] In a related study on palladium-catalyzed C(sp^2)−H activation, Ess et al. found a linear correlation between the C−H bond activation energy and the transition state Pd−C bond energy, demonstrating that the stability of the forming Pd−aryl bonds determines regioselectivity for a variety of arene and heteroarene substrates.[19]
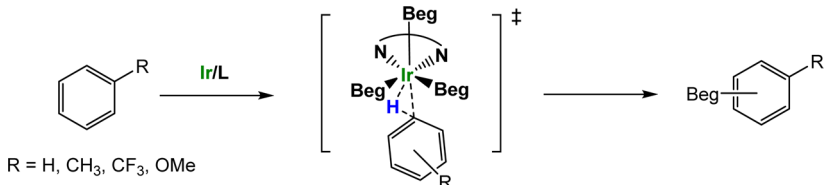
We recently employed the distortion/interaction model to investigate the origins of reactivity and selectivities in a variety of organic and organometallic reactions.[20−24] The distortion/interaction analysis has also been called the activation-strain model by Bickelhaupt.[25−27] In the distortion/interaction model, the activation energy ($\Delta E^\ddagger$) of a bimolecular process is divided into the energy to distort the reactants to the transition state

geometry ($\Delta E_{dist}^\ddagger$) and the energy of interaction between the distorted fragments ($\Delta E_{int}^\ddagger$). In a study on the Pd-catalyzed cross-coupling of polyhalogenated heterocycles, we reported that regioselectivities are controlled by both the energy to distort the C−X bond (related to BDE) and the interaction energy of the metal with the substrate.[21] In related studies, Gorelsky and Fagnou applied the distortion/interaction model to the palladium-catalyzed C−H activation of aromatic substrates involving the concerted metalation-deprotonation (CMD) mechanism.[28,29] They found that regioselectivity was determined by distortion energy or interaction energy or both depending on the substrate. Borovik and Shaik applied the distortion/interaction model to investigate the reactivity of C−H, N−H, and O−H bonds with nonheme iron oxo complexes and concluded the activation energy is mainly controlled by distortion energy, which they referred to as deformation energy.[30] Recently, Bickelhaupt et al. studied the palladium-induced activation of C−H, C−C, C−F, and C−Cl bonds in alkanes using the distortion/interaction (activation-strain) model.[31] They pointed out that the location of the transition state along the reaction coordinate has a large effect on the distortion and interaction energies and is an important consideration for understanding activation barriers. We have now for the first time applied the distortion/interaction model to study the factors that control regioselectivity of C−H oxidative additions in iridium-catalyzed borylations, and provide a model to understand the origins of selectivities in these reactions.

■ COMPUTATIONAL METHODS

Geometry optimizations were carried out using B3LYP and a mixed basis set of LANL2DZ for Ir and the double-ζ split-valence 6-31G(d) basis set for all other atoms. Vibrational frequency analysis confirmed that the structure was either a minimum or a transition state. Electronic energies were obtained from single-point calculations on the B3LYP geometries using Truhlar's M06 functional with a mixed basis set consisting of SDD for Ir and the triple-ζ split-valence 6-311G(d,p) basis set for other atoms. Solvation by *n*-octane was computed by single-point calculations using the SMD model. The nature of the C−H activation transition state for benzene was verified by intrinsic reaction coordinate (IRC) calculations which indicates this step leads to a phenyl Ir(V) hydride intermediate. The effectiveness of B3LYP for geometry optimizations and M06 for single-point energy calculations has been demonstrated by numerous studies to successfully produce energy profiles of reactions involving transition-metal complexes.[32−39] We examined the effects of dispersion in geometry optimizations. We found that the M06 activation energies computed using B3LYP or B3LYP-D for geometry optimizations were similar (see page S4 in the Supporting Information (SI)). All of the calculations in this study were performed

Table 1. Activation Energies and C−H/Ir−C Distances in the Oxidative Addition Transition States in C−H Borylation Reactions with Benzene and Monosubstituted Benzenes and the BDE of C−H Bonds in the Substrates

R = H, CH₃, CF₃, OMe

substrate	borylation position	exptl. product ratio	$\Delta G^{\ddagger}$ (kcal/mol)	$\Delta E^{\ddagger}$ (kcal/mol)	TS C−H length (Å)	TS Ir−C length (Å)	reactant C−H BDE (kcal/mol)
benzene		100	25.5	13.7	1.672	2.237	111.4
	o	0	28.2	14.6	1.742	2.276	109.7
1	m	69	25.6	13.6	1.670	2.236	109.5
	p	31	25.7	13.6	1.672	2.234	109.9
	o	0	25.7	12.1	1.676	2.228	113.1
2	m	70	23.1	11.0	1.640	2.234	112.3
	p	30	23.3	11.5	1.641	2.235	112.0
	o	1	26.4	14.5	1.662	2.242	111.0
3	m	74	24.7	12.8	1.676	2.238	111.1
	p	25	25.6	13.8	1.680	2.235	112.5

TS1-*o*
$\Delta G^{\ddagger}$ = 28.2 kcal/mol
$\Delta E_{(dist)}^{\ddagger}$(arene) = 68.7 kcal/mol

TS1-*m*
$\Delta G^{\ddagger}$ = 25.6 kcal/mol
$\Delta E_{(dist)}^{\ddagger}$(arene) = 66.0 kcal/mol

TS1-*p*
$\Delta G^{\ddagger}$ = 25.7 kcal/mol
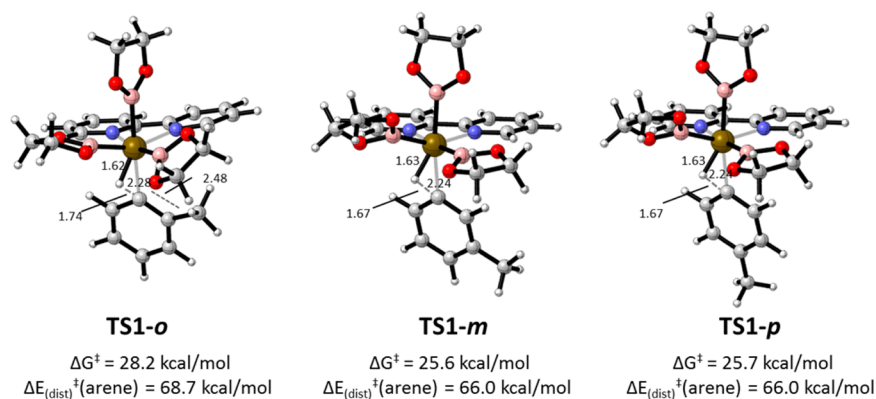$\Delta E_{(dist)}^{\ddagger}$(arene) = 66.0 kcal/mol

Figure 3. Oxidative addition transition states for the reaction of toluene, **1**. Activation free energies, and distortion energies of the substrate are given below each structure.

with Gaussian 09.[40] Compositions of molecular orbitals were calculated using the AOMix program.[41,42]

RESULTS AND DISCUSSION

The complex lacking the four methyl groups on each Bpin, (bpy)Ir(Beg)₃ (bpy = 2,2′-bipyridine; Beg = (ethyleneglycolato)boron)[9,17,43] was used as a model for (dtbpy)Ir(Bpin)₃. Although Beg is a poorer electron donor[44] and thus expected to be less reactive in C−H oxidative addition than the Bpin-ligated catalyst,[45] the effects on regioselectivity employing Beg in place of Bpin are expected to be small (see page S5 in the SI). The transition states for the C−H oxidative addition of these substrates have been calculated: benzene, three monosubstituted benzenes (**1−3**), three 1,2-disubstituted benzene rings (**4−6**), and seven 5-membered heterocycles (**7−13**).

Monosubstituted Benzene Rings. Substrates **1−3** have different electronic properties but similar steric properties. The activation energies for the rate- and regioselectivity-determining C−H activation step[8,9] are given in Table 1. The structures of the ortho, meta, and para C−H oxidative addition transition states for toluene **1** are shown in Figure 3 (**TS1-*o***, **TS1-*m***, and **TS1-*p***, respectively). The differences between the $\Delta G^{\ddagger}$ values (weighted Boltzmann average at 298 K: 1% ortho, 70% meta, and 29% para)

correspond well to the experimental selectivity (0% ortho, 69% meta, and 31% para). **TS1-*o*** is 2.5 kcal/mol less stable than the meta and para transition states, due to steric repulsions between the ortho methyl group of the substrate and the oxygen atom of one of the equatorial Beg groups (2.48 Å). Notably, the breaking C−H bond length for the ortho transition state (1.74 Å) is longer than the C−H bond length for the meta and para transition states (both are 1.67 Å), indicating that the ortho transition state is later than the meta and para transition states. Although being a later TS as indicated by the C−H bond length, the forming Ir−C bond is longer in the ortho transition state (2.28 Å) than those in meta- or para-transition states (both are 2.24 Å) due to the Beg−substrate steric repulsions. The relatively short Ir−C distances in all three regioisomeric transition states indicate that the transition state is late[46] and the Ir−C bond is almost fully formed.

As expected,[47] the activation energy for the more electron-poor trifluoromethylbenzene **2** is lower than that of toluene **1**, consistent with the experiment with a similar substrate 1,3-bis(trifluoromethyl)-benzene.[8] The trifluoromethyl group has an inverse electronic effect to that of the methyl group, but the relative meta/para selectivities of **1** and **2** remain the same. Borylation at the ortho positions of the monosubstituted benzene rings (**1**, **2**, and **3**) are all disfavored due to steric effects.

Table 2. Activation Energies and C−H/Ir−C Distances for the Oxidative Addition Transition States in C−H Borylation Reactions with 1,2-Disubstituted Benzenes and the BDE of C−H Bonds in the Substrates
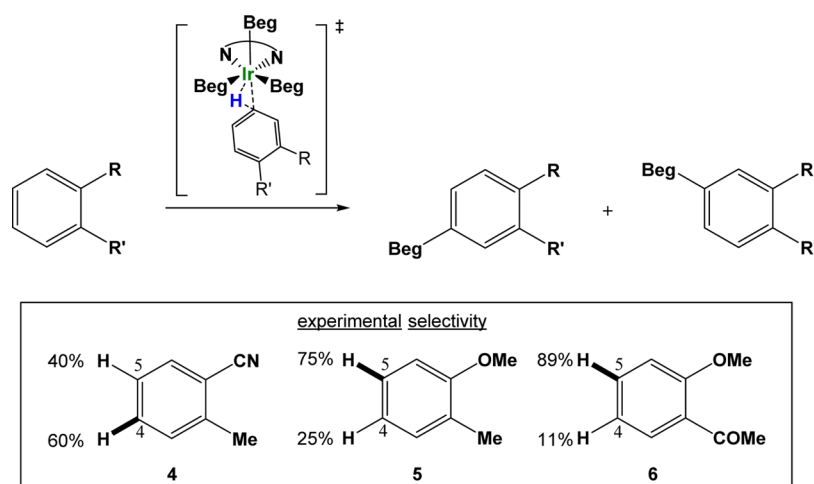
substrate	borylation position	exptl. product ratio	$\Delta G^{\ddagger}$ (kcal/mol)	$\Delta E^{\ddagger}$ (kcal/mol)	TS C−H length (Å)	TS Ir−C length (Å)	reactant C−H BDE (kcal/mol)
4	4	60	22.3	10.8	1.641	2.232	111.8
	5	40	22.8	11.2	1.631	2.236	112.6
5	4	25	26.2	14.0	1.688	2.234	112.3
	5	75	24.8	12.9	1.674	2.236	111.4
6	4	11	24.2	12.6	1.644	2.236	112.6
	5	89	23.2	11.1	1.658	2.231	111.3

Table 3. Activation Energies and C−H/Ir−C Distances for the Oxidative Addition Transition States in C−H Borylation Reactions with 5-Membered and Benzo-Fused Heterocycles and the BDE of C−H Bonds in the Substrates
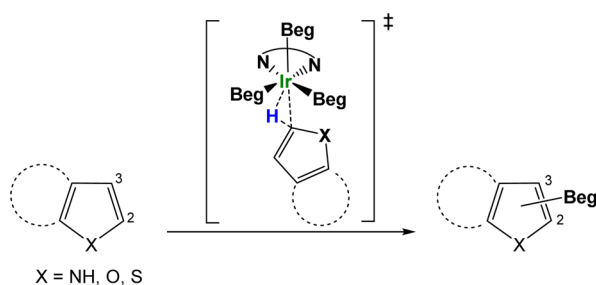
substrate	borylation position	exptl. product ratio	$\Delta G^{\ddagger}$ (kcal/mol)	$\Delta E^{\ddagger}$ (kcal/mol)	TS C−H length (Å)	TS Ir−C length (Å)	reactant C−H BDE (kcal/mol)
7	2	100	18.9	6.8	1.615	2.206	117.5
	3	0	23.6	11.8	1.717	2.234	114.1
8	2	100	16.9	5.6	1.597	2.206	116.8
	3	0	22.0	9.2	1.648	2.248	114.4
9	2	92	19.8	8.1	1.597	2.179	119.8
	3	7	24.2	12.8	1.703	2.214	118.7
10	2	97	18.2	6.9	1.569	2.177	119.3
	3	3	21.3	8.6	1.612	2.217	119.0
11	2	99	20.9	8.2	1.749	2.201	118.4
	3	0	25.5	13.7	1.686	2.209	117.6
12	2	76	26.2	13.1	1.725	2.223	118.6
	3	24	26.0	13.7	1.683	2.207	117.5
13	2	100	19.7	4.3	1.639	2.209	118.0
	3	0	26.1	11.6	1.664	2.216	118.3

1,2-Disubstituted Benzenes. The disubstituted benzenes, 1-methylbenzonitrile, 1-methoxy-2-methylbenzene, and 1-(2-methoxyphenyl)ethanone (**4**−**6**) all have sterically unhindered 4- and 5-positions, which only differ in electronic properties. Indeed, the C−H and Ir−C bond lengths in the transition state

structures for the activation of either the 4- or the 5-positions for **4**−**6** are similar suggesting that the steric effects are comparable (Table 2). The computed selectivities agree well with the experimental product ratios. In the case of **4**, there is little selectivity between the 4- and 5-positions. For both **5** and **6**,

activation at the 4-position leads to a slightly later transition state which coincides with a higher activation energy. Reactions occurring at the 3- and 6- positions were not computed, because steric effects prevent the reaction from occurring at these positions, as indicated in the calculations with monosubstituted benzenes.

We found the differences in selectivity for meta and para borylation are small for monosubstituted benzene derivatives and this agrees with the low selectivity observed experimentally. The meta:para selectivities for Ph−CH$_3$ (69:31) and Ph−CF$_3$ (70:30) are both very close to the 2:1 ratio of the number of meta and para C−H bonds. This indicates the electronic effects on regioselectivity are small for these monosubstituted benzenes. The electronic effects are only noticeable in 1,2-disubstituted cases with one strong electron donating group and one strong electron withdrawing group (8:1 ratio for substrate **6**). In the case of **6**, the C5-position has the largest orbital coefficient for the π^* orbital which presumably interacts with the metal d-orbital in the transition state.

5-Membered and Benzo-Fused Heterocycles. The 5-membered heterocycles predominantly borylate at the 2-position. Calculations correlate excellently with experimental regioselectivities (Table 3). In reaction with substrates **7**−**10**, the breaking C−H bond length is longer in the transition state for attack at the 3-position relative to the 2-position. The reverse trend is observed in substrates **11** and **12** where the activation at the 2-position occurs later (1.75 Å) than that at the 3-position (1.67 Å), but the 2-position is still favored energetically. Detailed analysis of the transition structure of **11** revealed hydrogen bonding between the N−H hydrogen of the pyrrole substrate and an oxygen atom of one of the Beg ligands, a result that was previously demonstrated by Smith and Singleton and is confirmed in this study (Figure S1).[43] Interestingly, the transition state of **12** is also late, even though hydrogen bonding cannot occur. This is likely due to steric repulsions with the methyl group on the nitrogen; the late transition state is stabilized by the favorable interaction of the metal and substrate at the electron-rich 2-position. Notably, the transition structure for the borylation of the 2-position of **13** does not exhibit hydrogen bonding and the transition state for the 2-borylation occurs earlier (1.64 Å) than in **11** or **12**.

Correlation between Activation Energy and Stability of the Aryl Iridium Hydride Intermediate. Recently, Smith and co-workers reported a good correlation between the activation barrier ($\Delta E^{\ddagger}$) and the energies of the intermediates after oxidative addition (ΔE_{rxn}) for iridium-catalyzed borylation reactions using the B3LYP/6-31G(d,p)-SDD method and (bpy)Ir(Beg)$_3$ as a model catalyst.[17] The correlation is indicative of a late transition state according to the Hammond-Leffler postulate.[48,49] The correlation is best when $\Delta E^{\ddagger}$ vs ΔE_{rxn} is plotted separately for arenes and heterocycles. We obtain similar correlation between $\Delta E^{\ddagger}$ and ΔE_{rxn} for **1**−**13** (Figure S2; R^2 = 0.85). The linear correlation increases dramatically when we do not include *N*-heterocycles in the analysis (Figure S3; R^2 = 0.94), similar to previous results by Smith et al.[17] The correlation between $\Delta E^{\ddagger}$ and ΔE_{rxn} may be due to the short Ir−C distance in the transition state. For example, the Ir−C distance in the transition structure for the C−H activation step of benzene is 2.24 Å and the Ir−C distance in the intermediate is very similar (2.15 Å) and as such, the stability of the transition state and the intermediate may both correlate with the Ir−C BDE.

Eisenstein et al. demonstrated that increasing Pd−aryl bond strengths in the product led to lower activation energies for Pd-catalyzed direct arylation of polyfluorinated benzenes which occurs through a concerted deprotonation-metalation (CMD) mechanism.[18] While they noted a good correlation of the activation energy with pK_a, an even better correlation to Pd−aryl bond strengths was observed.[18] We calculated the Ir−C BDEs for the aryl iridium hydride intermediates resulting from the C−H oxidative addition of **1**−**13**. A plot of $\Delta E^{\ddagger}$ vs Ir−C BDE for substrates **1**−**13** shows a definitive trend between the activation energy and the strength of the forming Ir−C bond; the stronger the Ir−C bond, the lower the activation energy for C−H activation (Figure 4). It might be expected that the correlation in
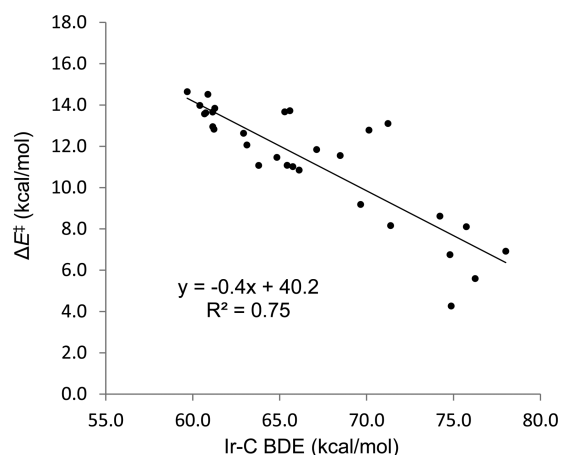
Figure 4. Plot of activation energies of C−H oxidative addition ($\Delta E^{\ddagger}$) vs Ir−C bond dissociation energies in the aryl iridium hydride intermediates for substrates **1**−**13**.

Figure 4 is only moderate (R^2 = 0.75). $\Delta E^{\ddagger}$ and Ir−C BDE represent properties of the transition state and the intermediate, respectively, and the correlation is affected by the position of the transition state on the reaction coordinate. However, the relative Ir−C BDE of different regioisomeric products is a useful tool to predict regioselectivities of the C−H activations. The relative strengths of the Ir−C bonds correctly predicted the regioselectivities for C−H activations of all substrates studied (see Table S1).

It has been proposed that the strength of metal−C bond may be affected by the polarity of the M−C covalent bonding; greater charge transfer from the metal, i.e., greater covalent-ionic (M$^+$C$^-$) resonance stability, leads to stronger a bond.[19,50,51] Indeed, Smith et al. have shown that more negatively charged aryl groups stabilize the aryl iridium intermediates.[17] In addition, we also observed a moderate correlation between the Ir−C bond strength and the energy needed to homolytically cleave the C−H bond (R^2 = 0.75; Figure S5), similar to the case for palladium.[18] At first glance, this correlation suggests that activation of the strongest C−H bond will occur since it will lead to the most stable Ir−C bond. While this trend sometimes holds true, there is no correlation between computed C−H BDEs and $\Delta E^{\ddagger}$ values (R^2 = 0.45, Figure S6). This indicates it is primarily the developing Ir−C bond and not the breaking C−H bond that determines relative activation energies.

Distortion/Interaction Analysis of the Transition States of 1−13. We explored the origins of reactivities and regioselectivities in the C−H activations of different substrates **1**−**13** using the distortion/interaction model (Table 4). The $\Delta E^{\ddagger}_{dist}$(Ir cat.) is the energy to distort the Ir and its ligands into the transition state geometry, while $\Delta E^{\ddagger}_{dist}$(arene) is the energy to

Table 4. Distortion/Interaction Analysis for the Oxidative Addition Transition States of 1−13[a]

substrate	borylation position	$\Delta E^{\ddagger}$	$\Delta E^{\ddagger}_{\text{dist}}$ (Ir cat.)	$\Delta E^{\ddagger}_{\text{dist}}$ (arene)	$\Delta E^{\ddagger}_{\text{int}}$	TS C−H length (Å)
benzene		13.7	11.2	65.9	−63.4	1.672
	o	14.6	11.8	68.7	−65.9	1.742
1	m	13.6	11.2	66.0	−63.6	1.670
	p	13.6	11.2	66.0	−63.6	1.672
	o	12.1	10.2	67.3	−65.4	1.676
2	m	11.0	10.9	62.8	−62.8	1.640
	p	11.5	11.0	63.1	−62.7	1.641
	o	14.5	11.0	67.4	−63.9	1.662
3	m	12.8	11.0	66.0	−64.2	1.676
	p	13.8	11.2	66.6	−64.0	1.680
4	4	10.8	10.8	63.0	−62.9	1.641
	5	11.1	10.7	61.8	−61.5	1.631
5	4	14.0	11.2	67.4	−64.6	1.688
	5	12.9	11.1	66.2	−64.3	1.674
6	4	12.6	10.9	64.5	−62.8	1.644
	5	11.1	10.9	63.7	−63.5	1.658
7	2	6.8	10.9	59.3	−63.5	1.615
	3	11.8	10.2	70.8	−69.2	1.717
8	2	5.6	10.8	57.5	−62.6	1.597
	3	9.2	10.6	64.3	−65.7	1.648
9	2	8.1	10.9	58.7	−61.5	1.597
	3	12.8	9.9	71.2	−68.3	1.703
10	2	6.9	10.8	56.0	−59.9	1.569
	3	8.6	10.6	61.0	−63.0	1.612
11	2	8.2	10.7	74.0	−76.5	1.749
	3	13.7	11.5	68.4	−66.2	1.686
12	2	13.1	10.3	72.8	−70.0	1.725
	3	13.7	11.7	68.1	−66.1	1.683
13	2	4.3	9.8	63.9	−69.4	1.639
	3	11.6	11.3	66.6	−66.3	1.664

[a]The activation energies, $\Delta E^{\ddagger}$, the distortion energies of the iridium catalyst, $\Delta E^{\ddagger}_{\text{dist}}$(Ir cat.), the distortion energies of the substrate, $\Delta E^{\ddagger}_{\text{dist}}$(**arene**), and the interaction energies, $\Delta E^{\ddagger}_{\text{int}}$, are given in kcal/mol.

Figure 5. Plot of substrate distortion energy ($\Delta E^{\ddagger}_{\text{dist}}$(arene)) versus the C−H bond length in the transition state.

distort the arene substrate into the transition state geometry. $\Delta E^{\ddagger}_{\text{int}}$ is the energy of interaction between these distorted fragments. The distortion energies of the iridium catalyst in all reactions are very similar, typically within ±1 kcal/mol of that in the reaction with benzene (11.2 kcal/mol). Thus, the distortion of the catalyst does not noticeably affect the regioselectivities of C−H activation. The energy required to distort the aromatic substrates into the transition state geometry ($\Delta E^{\ddagger}_{\text{dist}}$(arene)) correlates well with the C−H bond distance in the transition state (Figure 5, R^2 = 0.92), indicating that the distortion energy is mainly controlled by the position of the transition state on the reaction coordinate. The distortion energy does not correlate well with the activation energy or the strength of the C−H bond in the substrate (see Figures S4 and S9). This indicates that substrate distortion is not the major factor that controls regioselectivities.

There is no obvious correlation between the interaction energy and the activation energy (Figure S8), as the interaction energy between the substrate and the catalyst in the transition state is also affected by the early or late location of the transition state. For example, in the reaction with thiophene (**7**), the interaction energy for the C3-activation (−69.2 kcal/mol) is much greater than that for the C2-activation (−63.5 kcal/mol), although the C−H activation occurs exclusively at the 2-position.
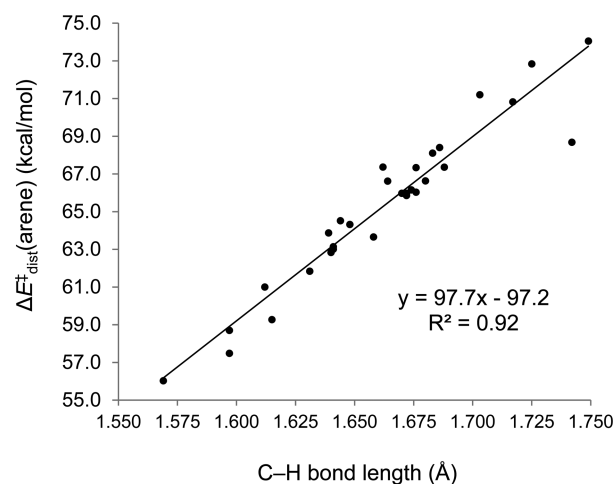
This is due to the much earlier transition state for C2-activation. Similarly, in reactions with heterocycles **8−10**, interaction energies for C3-activations are greater than those for C2-activations due to the much later transition states in the C3-activation pathway. The trend is reversed in the reaction with pyrrole (**11**), in which the large interaction energy for the activation at the 2-position (−76.6 kcal/mol) is partly due to hydrogen bonding of the N−H hydrogen with one of the oxygen atoms on an equatorial Beg ligand (O−H bond length of 1.98 Å) as mentioned previously. A higher energy conformer of the transition state was found that did not exhibit hydrogen bonding and the interaction energy (−66.8 kcal/mol) was similar to the interaction energy for activation at the 3-position (−66.2 kcal/mol).

In order to understand the effect of an early vs late transition state on the distortion and interaction energies, we performed a distortion/interaction analysis along the reaction coordinate for C2 and C3-activations of thiophene (**7**; Figure 6; for **1** and **6**, see Figures S13 and S14, respectively). The data points for each geometry along the reaction coordinate were obtained by performing a relaxed scan of the breaking C−H bond from 1.350 to 1.900 Å in intervals of 0.025 Å. The total energy, distortion energy, and interaction energy for each point along the reaction paths were computed. As discussed earlier, the distortion energies of the iridium catalyst are very similar along the two different reaction paths, and thus are not plotted in Figure 6. The total energy curve along each reaction path is relatively flat in the transition state region. This explains why the locations of the transition states are easily affected by the C2 or C3 activations. In all three reactions investigated, the distortion energy becomes more positive and the interaction energy becomes more negative when increasing the breaking C−H bond length. At all points along the reaction coordinate with thiophene (**7**), the difference between distortion energies for the C2 and C3 activations is relatively small (<4 kcal/mol). However, at all points along the reaction coordinate, the interaction energy for the 2-activation is significantly greater than the 3-activation (>6 kcal/mol). Since the transition state for 2-borylation is much earlier than 3-borylation, the interaction energy of the 2-borylation TS is smaller than the 3-borylation TS (−63.5 and −69.2 kcal/mol for 2- and 3-positions, respectively). Nonetheless, the dramatic difference of interaction energies between 2- and 3-activations along the reaction coordinate indicates the origin of the high
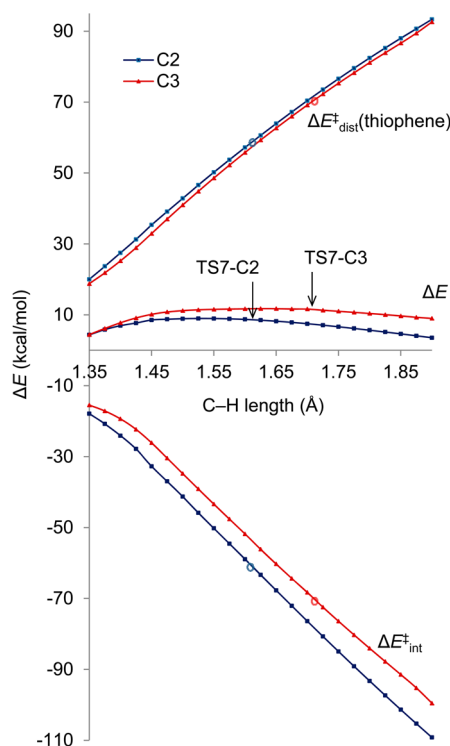
Figure 6. Energy (ΔE), substrate distortion energy ($\Delta E^{\ddagger}_{dist}$(thiophene)) and interaction energy of thiophene with iridium complex (ΔE_{int}) as a function of the breaking C−H bond length in the reaction of thiophene **7**.

Figure 7. Plot of activation energy $\Delta E^{\ddagger}$ vs transition state Ir−C bond energy ΔE_{tbe} for reactions with **1−13**.

selectivity of 2-borylation is the greater interaction energy between the catalyst and the substrate. This is a case for which, as Bickelhaupt pointed out, simply using the interaction energies at the transition states is not adequate to describe the effects of distortions and interactions, due to the effects of different locations of the isomeric transition states on the reaction coordinate.[31] Similar results were obtained for substrates **1** and **6** (see the SI). These results indicate that Ir−substrate interaction energy is the driving factor in the respective selectivities for the C−H activation of **1−13**. This agrees with the correlation between activation energy and the Ir−aryl bond strength discussed earlier.

In order to understand the origins of the differences of the interaction energies, we probed a number of different factors. Interaction energies have previously been explained on the basis HOMO−LUMO interactions between the substrate and the catalyst. However, analysis of the fragment orbital contributions between thiophene and Ir(bpy)(Beg)$_3$ shows that these interactions are complex (Figure S15) and simple arguments based on secondary orbital overlap are not feasible.

To quantify more directly how the iridium−aryl bonding interaction influences the activation energy, we calculated the TS Ir−C bond energies,[19] ΔE_{tbe}, for **1−13**. Figure 7 illustrates how we define the TS Ir−C bond energies, following the approach of Ess.[19] This involves calculation of the Ir−C bond energy at the transition state structure without geometry relaxation ([Ir(bpy)-(Beg)$_3$(Ar)]$^{\ddagger} \rightarrow$ [Ir(bpy)(Beg)$_3 \bullet$]‡ + [Ar$\bullet$]‡). Figure 7 also shows a plot of $\Delta E^{\ddagger}$ vs ΔE_{tbe} for the activation of all C−H bonds in arenes and heteroarenes **1−13**. There is a good linear correlation ($R^2 = 0.81$) between these values, which reveals that the Ir−C bonding interaction that develops along the reaction coordinate for C−H bond activation contributes significantly to
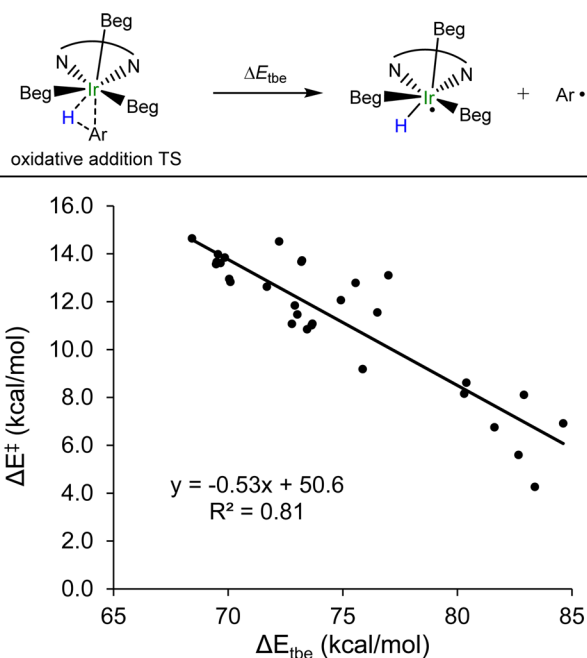
stabilizing the TS and determines regioselectivity. Indeed, deviation from a perfect linear correlation is expected, due to the differences in early vs late C−H activation on the reaction coordinate for the respective positions activated in **1−13**. Notably, removal of the nitrogen heterocycle substrates leads to improved correlation between $\Delta E^{\ddagger}$ and ΔE_{tbe} ($R^2 = 0.87$; Figure S10).

Three substrates, PhBpin **15**, benzodioxole **16**, and 4-fluorobenzonitrile **17**, were examined to further test the relationship between $\Delta E^{\ddagger}$ and ΔE_{tbe} (Scheme 2). In the case of

Scheme 2. Experimental Selectivities of Borylation of 15−17
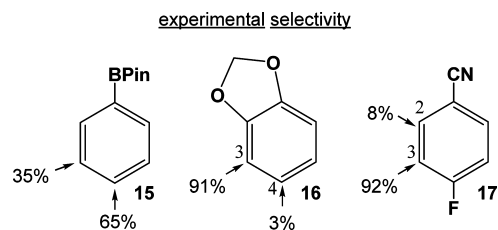
15, the observed experimental selectivity (determined by GC) for borylation at the para position is low; however, the para position is slightly favored on the order of 35%:65% (meta/para).[52] The computed C−H activation energies are 25.3 and 25.5 kcal/mol for the meta and para borylation of **15**, respectively. Our computations are in reasonable agreement with experiment and predict low selectivity for meta vs para borylation of **15**. Our computed activation energies for **16** (23.0 and 25.5 kcal/mol for 3- and 4-borylation, respectively; predicted selectivity 98.5%:1.5%) also agree well with Smith's experimental observations for the borylation of benzodioxole.[17] Experimentally, 91% and 3% 3- and 4-borylation products are observed with **16**, along with 6% diborylated product.[17] Computed activation energies for the C−H activation of **17** at 2- and 3-positions are 18.4 and 16.1 kcal/mol, respectively (predicted selectivity 2%:98%). Experimentally, Smith et al. showed that borylation

of **17** leads to high selectivity for the 3-position, i.e., ortho to the fluorine group (2-:3-borylation 8%:92%, isolated yield).[52] The selectivity in the reactions with **15**-**17** is also controlled by the Ir−C BDEs. Correlation between $\Delta E^{\ddagger}$ and Ir−C BDE for **1**−**13** and **15**−**17** ($R^2 = 0.73$) is similar to the previously obtained correlation for **1**−**13** (see Figure S11). Additionally, plotting $\Delta E^{\ddagger}$ vs ΔE_{tbe} for the activation of all computed C−H bonds in arenes and heteroarenes **1**−**13** and **15**−**17** leads to a good linear correlation ($R^2 = 0.81$) (see Figure S12).

CONCLUSION

We have studied the origins of regioselectivity in iridium-catalyzed C−H borylation reaction of substituted benzene rings and heterocycles. Distortion/interaction analyses show that regioselectivity is determined primarily by the interaction energy between the iridium catalyst and the substrate in the oxidative addition transition state. As a result, Ir−C bond energies in the aryl iridium hydride intermediates or in the C−H oxidative addition transition states both correlate well with the activation energy and can be used to determine the regioselectivity of the C−H activation reaction.

ASSOCIATED CONTENT

Ⓢ Supporting Information

Complete ref 40, optimized geometries, and energies of all computed species. This material is available free of charge via the Internet at http://pubs.acs.org.

AUTHOR INFORMATION

Corresponding Author

houk@chem.ucla.edu; merlic@chem.ucla.edu

Notes

Notes. The authors declare no competing financial interest.

ACKNOWLEDGMENTS

REFERENCES

(1) Godula, K.; Sames, D. *Science* **2006**, *312*, 67.
(2) Davies, H. M. L.; Manning, J. R. *Nature* **2008**, *451*, 417.
(3) Brown, H. C. *Organic Syntheses via Boranes*; Wiley: New York, 1975.
(4) Pelter, A.; Smith, K.; Brown, H. C. *Borane Reagents*; Academic Press: Ann Arbor, MI, 1988.
(5) Ishiyama, T.; Miyaura, N. *Pure Appl. Chem.* **2006**, *78*, 1369.
(6) Mkhalid, I. A. I.; Barnard, J. H.; Marder, T. B.; Murphy, J. M.; Hartwig, J. F. *Chem. Rev.* **2010**, *110*, 890.
(7) Hartwig, J. F. *Acc. Chem. Res.* **2012**, *45*, 864.
(8) Boller, T. M.; Murphy, J. M.; Hapke, M.; Ishiyama, T.; Miyaura, N.; Hartwig, J. F. *J. Am. Chem. Soc.* **2005**, *127*, 14263.
(9) Tamura, H.; Yamazaki, H.; Sato, H.; Sakaki, S. *J. Am. Chem. Soc.* **2003**, *125*, 16114.
(10) An excellent complementary study on the origins of regioselectivity in the iridium-catalyzed borylation of heterocycles was published while this manuscript was under revision. Larsen, M. A.; Hartwig, J. F. *J. Am. Chem. Soc.* DOI: 10.1021/ja412563e. Published online: Feb, 7, **2014**.

(11) Ishiyama, T.; Takagi, J.; Ishida, K.; Miyaura, N.; Anastasi, N. R.; Hartwig, J. F. *J. Am. Chem. Soc.* **2002**, *124*, 390.
(12) Ishiyama, T.; Takagi, J.; Hartwig, J. F.; Miyaura, N. *Angew. Chem., Int. Ed.* **2002**, *41*, 3056.
(13) Ishiyama, T.; Nobuta, Y.; Hartwig, J. F.; Miyaura, N. *Chem. Commun.* **2003**, 2924.
(14) Tajuddin, H.; Harrisson, P.; Bitterlich, B.; Collings, J. C.; Sim, N.; Batsanov, A. S.; Cheung, M. S.; Kawamorita, S.; Maxwell, A. C.; Shukla, L.; Morris, J.; Lin, Z.; Marder, T. B.; Steel, P. G. *Chem. Sci.* **2012**.
(15) Ishiyama, T.; Takagi, J.; Yonekawa, Y.; Hartwig, J. F.; Miyaura, N. *Adv. Synth. Catal.* **2003**, *345*, 1103.
(16) Takagi, J.; Sato, K.; Hartwig, J. F.; Ishiyama, T.; Miyaura, N. *Tetrahedron Lett.* **2002**, *43*, 5649.
(17) Vanchura, B. A., II; Preshlock, S. M.; Roosen, P. C.; Kallepalli, V. A.; Staples, R. J.; Maleczka, J. R. E.; Singleton, D. A.; Smith, M. R., III *Chem. Commun.* **2010**, *46*, 7724.
(18) Guihaume, J.; Clot, E.; Eisenstein, O.; Perutz, R. N. *Dalton Trans.* **2010**, *39*, 10510.
(19) Petit, A.; Flygare, J.; Miller, A. T.; Winkel, G.; Ess, D. H. *Org. Lett.* **2012**, *14*, 3680.
(20) Ess, D. H.; Houk, K. N. *J. Am. Chem. Soc.* **2007**, *129*, 10646.
(21) Legault, C. Y.; Garcia, Y.; Merlic, C. A.; Houk, K. N. *J. Am. Chem. Soc.* **2007**, *129*, 12664.
(22) Ess, D. H.; Houk, K. N. *J. Am. Chem. Soc.* **2008**, *130*, 10187.
(23) Hayden, A. E.; Houk, K. N. *J. Am. Chem. Soc.* **2009**, *131*, 4084.
(24) Schoenebeck, F.; Ess, D. H.; Jones, G. O.; Houk, K. N. *J. Am. Chem. Soc.* **2009**, *131*, 8121.
(25) van Zeist, W.-J.; Bickelhaupt, F. M. *Org. Biomol. Chem.* **2010**, *8*, 3118.
(26) Fernández, I.; Cossío, F. P.; Bickelhaupt, F. M. *J. Org. Chem.* **2011**, *76*, 2310.
(27) Fernández, I.; Bickelhaupt, F. M. *J. Comput. Chem.* **2012**, *33*, 509.
(28) Gorelsky, S. I.; Lapointe, D.; Fagnou, K. *J. Org. Chem.* **2011**, *77*, 658.
(29) Gorelsky, S. I.; Lapointe, D.; Fagnou, K. *J. Am. Chem. Soc.* **2008**, *130*, 10848.
(30) Usharani, D.; Lacy, D. C.; Borovik, A. S.; Shaik, S. *J. Am. Chem. Soc.* **2013**, *135*, 17090.
(31) de Jong, G. T.; Bickelhaupt, F. M. *ChemPhysChem* **2007**, *8*, 1170.
(32) Benitez, D.; Tkatchouk, E.; Goddard, W. A., III *Chem. Commun.* **2008**, 6194.
(33) Lin, M.; Kang, G.-Y.; Guo, Y.-A.; Yu, Z.-X. *J. Am. Chem. Soc.* **2011**, *134*, 398.
(34) Zhou, M.; Balcells, D.; Parent, A. R.; Crabtree, R. H.; Eisenstein, O. *ACS Catal.* **2011**, *2*, 208.
(35) Tang, S.-Y.; Guo, Q.-X.; Fu, Y. *Chem.—Eur. J.* **2011**, *17*, 13866.
(36) Yeom, H.-S.; Koo, J.; Park, H.-S.; Wang, Y.; Liang, Y.; Yu, Z.-X.; Shin, S. *J. Am. Chem. Soc.* **2011**, *134*, 208.
(37) Liu, P.; Xu, X.; Dong, X.; Keitz, B. K.; Herbert, M. B.; Grubbs, R. H.; Houk, K. N. *J. Am. Chem. Soc.* **2012**, *134*, 1464.
(38) Giri, R.; Lan, Y.; Liu, P.; Houk, K. N.; Yu, J.-Q. *J. Am. Chem. Soc.* **2012**, *134*, 14118.
(39) Herbert, M. B.; Lan, Y.; Keitz, B. K.; Liu, P.; Endo, K.; Day, M. W.; Houk, K. N.; Grubbs, R. H. *J. Am. Chem. Soc.* **2012**, *134*, 7861.
(40) Frisch, M. J.; et al. *Gaussian 09*, revision B.01; Gaussian, Inc.: Wallingford CT, 2009.
(41) Gorelsky, S. I.; Lever, A. G. P. *J. Organomet. Chem.* **2001**, *635*, 187.
(42) Gorelsky, S. I. *AOMix: Program for Molecular Orbital Analysis*, version 6.8, http://www.sg-chem.net, Ottawa, ON. 2013.
(43) Roosen, P. C.; Kallepalli, V. A.; Chattopadhyay, B.; Singleton, D. A.; Maleczka, R. E.; Smith, M. R., III *J. Am. Chem. Soc.* **2012**, *134*, 11350.
(44) Zhu, J.; Lin, Z.; Marder, T. B. *Inorg. Chem.* **2005**, *44*, 9384.
(45) Liskey, C. W.; Wei, C. S.; Pahls, D. R.; Hartwig, J. F. *Chem. Commun.* **2009**, 5603.
(46) Here we define position of the transition state using the Ir−C bond as reaction coordinate.
(47) Hartwig, J. F. *Organotransition Metal Chemistry: From Bonding to Catalysis*; University Science Books: Sausalito, CA, 2010.
(48) Leffler, J. E. *Science* **1953**, *117*, 340.

(49) Hammond, G. S. *J. Am. Chem. Soc.* **1955**, *77*, 334.

(50) Sakaki, S.; Biswas, B.; Sugimoto, M. *Organometallics* **1998**, *17*, 1278.

(51) Sakaki, S.; Kai, S.; Sugimoto, M. *Organometallics* **1999**, *18*, 4825.

(52) Chotana, G. A.; Rak, M. A.; Smith, M. R., III *J. Am. Chem. Soc.* **2005**, *127*, 10539.

4583

dx.doi.org/10.1021/ja411699u | *J. Am. Chem. Soc.* 2014, 136, 4575−4583